

^{119}Sn NMR probe of magnetic fluctuations in SnO_2 nanoparticles

Tusharkanti Dey,* P. Khuntia, and A.V. Mahajan

Department of Physics, Indian Institute of Technology Bombay, Powai, Mumbai 400076, India

Nitesh Kumar and A. Sundaresan

Jawaharlal Nehru Centre for Advanced Scientific Research (JNCASR), Jakkur P. O., Bangalore 560064, India

Abstract

^{119}Sn nuclear magnetic resonance (NMR) spectra and spin-lattice relaxation rate ($1/T_1$) in SnO_2 nanoparticles were measured as a function of temperature and compared with those of SnO_2 bulk sample. A 15% loss of ^{119}Sn NMR signal intensity for the nano sample compared to the bulk sample was observed. This is indicative of ferromagnetism from a small fraction of the sample. Another major finding is that the recovery of the ^{119}Sn longitudinal nuclear magnetization in the nano sample follows a stretched exponential behavior, as opposed to that in bulk which is exponential. Further, the ^{119}Sn $1/T_1$ at room temperature is found to be much higher for the nano sample than for its bulk counterpart. These results indicate the presence of magnetic fluctuations in SnO_2 nanoparticles in contrast to the bulk (non-nano) which is diamagnetic. These local moments could arise from surface defects in the nanoparticles.

PACS numbers: 75.50.Pp, 75.50.Dd, 76.60.-k, 75.75.Jn

Introduction. - The discovery of ferromagnetism even for dilute doping in semiconductors and insulators has been one of the biggest surprises for researchers. In 1998, H. Ohno [1] reported the observation of ferromagnetism in Mn doped GaAs with a Curie temperature as high as 110K. After two years, T. Dietl *et al.* [2] first predicted the possible appearance of ferromagnetism above room temperature in Mn doped ZnO and GaN. After that many researchers put great effort to find a room temperature, intrinsic, dilute magnetic semiconductor (DMS). Thin films and bulk samples of transition metal doped metal oxides like TiO_2 , ZnO, In_2O_3 , SnO_2 , and CeO_2 were found to show ferromagnetism [3–7] at room temperature. More interestingly, thin films of a band insulator HfO_2 , which is diamagnetic in bulk form, was found to be ferromagnetic without any doping, with Curie temperature greater than 500K [8]. Thereafter, many *undoped*, wide band gap, semiconductor metal oxides such as TiO_2 , ZnO, SnO_2 , In_2O_3 , Al_2O_3 , CeO_2 , etc. were found to show room temperature ferromagnetism in nanoparticulate or thin film form [9–11]. Sundaresan *et al.* [9] suggested that all metal oxides in nanoparticulate form would exhibit room temperature ferromagnetism. All these discoveries of ferromagnetism in semiconducting or insulating oxides without any unpaired ‘*d*’ or ‘*f*’ electron have questioned the basic understanding of the origin of magnetism [8].

Sundaresan *et al.* [9] argued that oxygen vacancies at the surfaces are responsible for ferromagnetism in CeO_2 , Al_2O_3 , ZnO, In_2O_3 , and SnO_2 nanoparticles. From *ab initio* density functional calculations, Ganguli *et al.* [12] argued that defects in ZnO clusters even in the absence of transition metal doping may drive the cluster magnetic. Using density functional theory, Rahman *et al.* [13] observed that in SnO_2 nanoparticles oxygen vacancy

is nonmagnetic but a tin vacancy is ferromagnetic with a large magnetic moment and coupled strongly with other Sn defects. In another study by first principles calculation, Wang *et al.* [14] have concluded that surface defects are responsible for ferromagnetism in undoped SnO_2 nanoparticles. All these studies infer that defects at the surface play a key role in ferromagnetism in SnO_2 nanoparticles.

Nuclear magnetic resonance (NMR) is widely used for detecting magnetic fluctuations, crystal environment etc. at a local level in bulk materials. NMR is also used to study nano materials [15–18]. Tang *et al.* [16] have measured ^{67}Zn NMR in ZnS nanoparticles. They reported no detectable NMR signal due to quantum size effects when the average particle size was below 4 nm and signal was observed when average particle size was more than 8 nm. Monredon *et al.* [18] performed ^{119}Sn MAS NMR on nanoparticles of SnO_2 of different sizes to show that the spectral shape change with the average size of the nanoparticles. Sabarinathan *et al.* [15] also performed ^{119}Sn MAS NMR on SnO_2 nanoparticles to measure spectra as well as spin-spin and spin-lattice relaxations for two samples of different particle size. Their study shows that smaller the size of the particles, faster is the relaxation. They concluded that inhomogeneous broadening of the spectra is due to the surface defects of the nanocrystalline samples. However, the spin-lattice relaxation analysis by them is not reliable due to the lack of optimal measurement parameters [19]. According to our knowledge, no detailed NMR measurement on ferromagnetic metal oxide nanoparticles is reported so far.

With the motivation of verifying the presence of local moments in nanoparticles via a local probe, we have chosen SnO_2 as a representative candidate for detailed NMR measurements. We have measured ^{119}Sn NMR spectra and spin-lattice relaxation time at different temperatures for the SnO_2 nano sample and compared them with those in the SnO_2 bulk sample. We observed a 15% loss of the ^{119}Sn NMR spectral intensity in the nano sample when

*Email: tusdey@gmail.com

compared with the bulk. This is likely due to static, local magnetic moments on a fraction of Sn atoms. This could very well be due to (possibly defect induced) ferromagnetic surfaces of the smaller nanoparticles. The large local field at these ^{119}Sn nuclei will shift the resonance out of the window of our observation. Non single-exponential recoveries obtained for the nano sample in spin-lattice relaxation measurements are probably due to the distribution of relaxation rates from different paramagnetic layers in the nanoparticles. The faster relaxation rate for the nano sample compared to the bulk sample indicates the presence of magnetic fluctuations in the nano sample.

Experimental details. - SnO_2 nanoparticles were prepared at JNCASR by a modified synthetic procedure discussed by Gnanam *et al.* [20]. In a typical synthesis, 2.5 g of SnCl_2 was dissolved in ethanol to get a clear solution. 6 mL ammonia (30%) was added slowly to the above solution with constant stirring to get a white precipitate. The precipitate was centrifuged and washed with distilled water several times till the pH became 7 followed by the last washing with ethanol. The white product was dried at 80°C for 5 h. After drying, the product became yellow. The yellow powder was heated at 450°C in oxygen atmosphere for two hours to get crystalline nanoparticles of SnO_2 . The bulk sample was prepared by pelletizing the powder and sintering the cylindrical pellet at 1100°C for 24 h.

X-ray diffraction (XRD) patterns were collected with a Rigaku-99 diffractometer using $\text{Cu } K_\alpha$ radiation ($\lambda = 1.5406\text{\AA}$). Transmission electron microscopy (TEM) images were recorded with a JEOL JEM 3010 instrument (Japan) operated with an accelerating voltage of 300 kV. Magnetic measurements were carried out using a Quatum Design Physical Property Measurement System (PPMS).

After these basic characterizations, we have carried out ^{119}Sn NMR measurements for both bulk and nano samples of SnO_2 at IIT Bombay. Sn has three NMR active isotopes (^{115}Sn , ^{117}Sn , and ^{119}Sn). Our measurements are on the ^{119}Sn nucleus ($I = 1/2$) because it has the highest $\gamma/2\pi$ value (15.869 MHz/T) and the highest natural abundance (8.58%) among the three. For NMR measurements we have used a Tecmag pulse spectrometer and a fixed magnetic field 93.954 kOe obtained inside a room temperature bore Varian superconducting magnet. Variable temperature measurements were carried out with the help of an Oxford cryostat and accessories. Spin lattice relaxation was measured using a standard saturation recovery method following a $\pi/2 - t - (\pi/2 - \pi)$ pulse sequence where the typical $\pi/2$ pulse width was $6\mu\text{s}$.

Results and discussions. - Figure 1 shows XRD patterns of nanoparticles as well as bulk SnO_2 . The nanoparticles as well as bulk powder crystallize in a tetragonal rutile structure. Using Scherrer's formula for the XRD peak broadening we obtain the particle size to be $\sim 13\text{ nm}$.

Figure 2 shows TEM images of SnO_2 nanoparticles. Histogram of size distribution is shown in the inset of

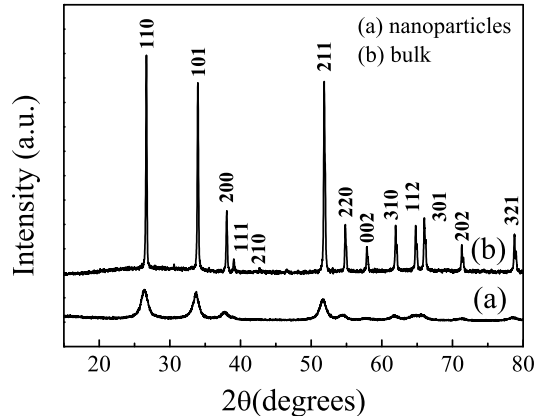


Figure 1: XRD patterns of (a) nanoparticles and (b) bulk SnO_2 sample.

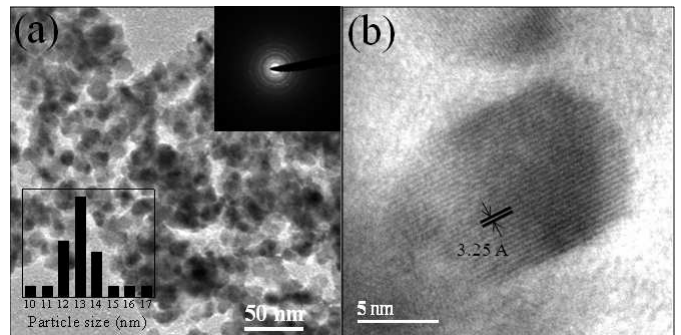


Figure 2: (a) TEM image of SnO_2 nanoparticles. The two insets show the particle size distribution and the ED pattern, (b) HRTEM image of a SnO_2 nanoparticle.

fig. 2(a). Average particle size was found to be $\sim 13\text{ nm}$ which matches with the value calculated from XRD peak broadening. Rings in electron diffraction (ED) pattern shown in the inset of fig. 2(a) confirm the particles to be polycrystalline in nature. Figure 2(b) shows high resolution TEM image of a SnO_2 nanoparticle. Lattice fringes corresponding to the (110) planes can be seen clearly.

Figure 3 shows magnetic hysteresis loops for the SnO_2 nano sample as well as magnetization isotherms for bulk SnO_2 sample at different temperatures. As expected, the bulk SnO_2 sample simply shows diamagnetic M vs H isotherms. On the other hand, SnO_2 nanoparticles show ferromagnetic hysteresis loops with saturation magnetization (M_S) value of $\sim 2 \times 10^{-4}$ ($\mu_B/\text{formula unit}$). This value was calculated taking the total mass of the nanoparticles. However, ferromagnetism in SnO_2 nanoparticles is believed to be a surface effect and taking only the 'surface' mass (corresponding to a one unit cell thick spherical shell of diameter 13 nm), M_S will be $\sim 10^{-3}$ ($\mu_B/\text{formula unit}$).

Clearly this bulk technique measures an average of all the magnetic moments in the sample. In the present case

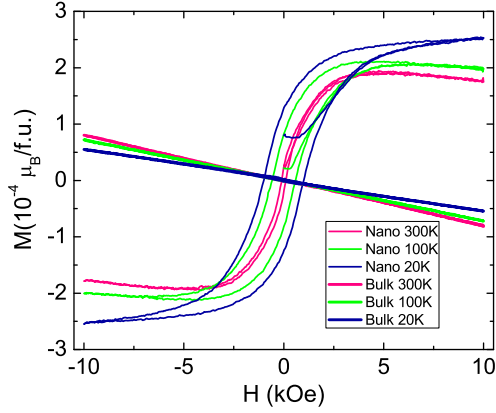


Figure 3: (Color online) Magnetic hysteresis loops for the SnO₂ nano sample (thin curves) and magnetization isotherms for the bulk sample (thick curves) at various temperatures are shown after subtracting the diamagnetic holder contribution.

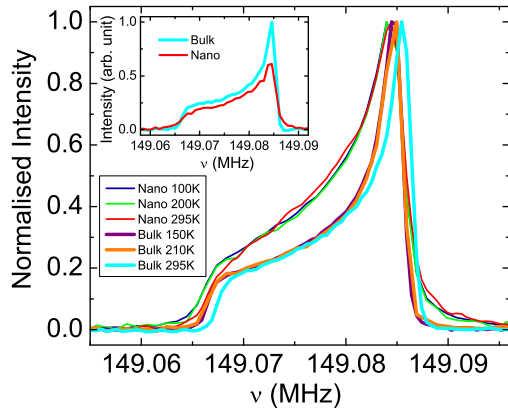


Figure 4: (Color online) Spectra of SnO₂ bulk (thick lines) and nano sample (thin lines) at different temperatures. Inset: Comparison of spectra of bulk and nano sample of SnO₂ at room temperature measured with identical parameters and normalised to mass.

there is bound to be a distribution of moments; the atoms of the surface having a greater moment than the core and this distribution possibly being further dependent on the size of the particles.

Our ¹¹⁹Sn NMR measurements provide a local probe of this magnetism. The total ¹¹⁹Sn NMR spectral intensity is found to be smaller in the nano sample compared to the bulk (see inset of fig. 4) by about 15%. This loss could arise due to static moments on Sn atoms which provide a large magnetic field at the ¹¹⁹Sn nucleus (typical hyperfine coupling $\sim 40 \text{ kOe}/\mu_B$ [21]) and move the NMR signal out of our window of observation.

The NMR lineshape for the nano sample is somewhat broader than for the bulk and unchanged with temper-

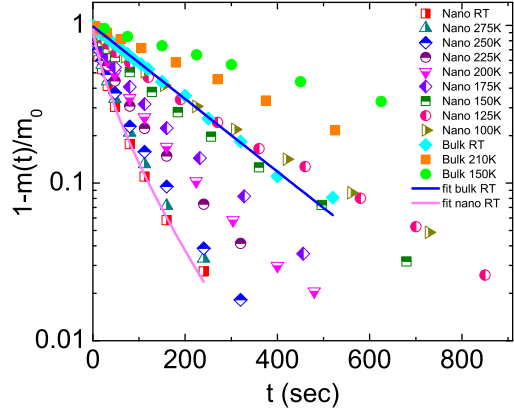


Figure 5: (Color online) Spin-lattice relaxation recovery curves of the SnO₂ bulk (solid symbols) and nano sample (half-filled symbols) at different temperatures. Fitting of the recovery data with stretched exponential for nano sample and exponential for bulk sample (both as solid lines) at room temperature (RT) are also shown.

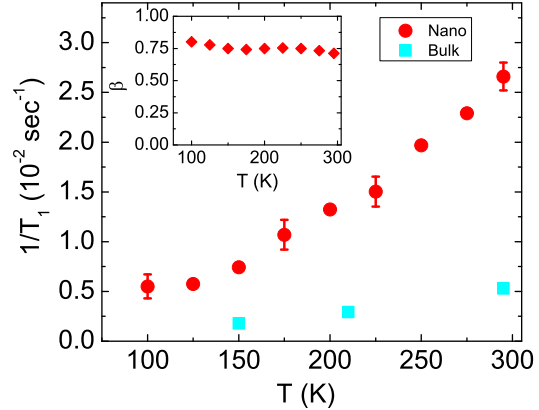


Figure 6: (Color online) Relaxation rates obtained by fitting the recoveries of SnO₂ nano sample with Eq. 1 plotted as a function of temperature T . The light blue squares indicate the relaxation rates of the bulk sample. Inset: The temperature variation of the exponent β obtained from fitting of recovery data with Eq. 1.

ature (see fig. 4). The increase in width (full width at half maxima increases from about 4 kHz to about 7 kHz and total extent of spectra increases from about 21 kHz to about 25 kHz) could arise from a distribution of anisotropy (surface vs core). The total spectral intensity (corrected for temperature and T_2 effects) is found independent of temperature for the nano sample. This implies that the total no. of ¹¹⁹Sn nuclei that we probe does not change with temperature or parts of the sample do not progressively become ferromagnetic as temperature decreases.

We next focus on the spin-lattice relaxation rate data. The recovery of the ^{119}Sn nuclear magnetisation following a $\pi/2$ pulse is shown in fig. 5 for the nano and the bulk samples at various temperatures. As expected, for the $I = 1/2$ ^{119}Sn nucleus, the nuclear magnetic recovery for the bulk sample is exponential with an extremely long T_1 (~ 180 s) at room temperature. For this sample, the T_1 increases to about 560 s by 150 K and is expected to increase further at lower temperature. Here, the relaxation probably arises from a coupling to lattice vibrations typical in nonmagnetic insulators. In contrast, for the nano sample, the recovery is not single-exponential. However, we could fit the recovery at all temperatures to a stretched exponential function

$$1 - m(t)/m_0 = \exp[-(t/T_1)^\beta] \quad (1)$$

where the β is nearly unchanged with temperature (see inset of fig. 6). The $1/T_1$ thus obtained is plotted in fig. 6. The faster relaxation rate for the nano sample must then arise from fluctuating paramagnetic moments at Sn sites. A distribution in the value of such magnetic moments (higher near the surface, smaller in the core, and perhaps grain size dependent) then leads to a distribution of T_1 . Note that the longest T_1 component as obtained from the slope of the data (at 300 K for the nano sample) at high- t in fig. 5 is about 80 s which is still less than half the value for the bulk. For a paramagnet, the spin-lattice relaxation rate is expected to be nearly T -independent at high- T and might increase a little with a decrease in temperature. The decrease in $1/T_1$ seen by

us points to a gap in the spin excitation spectrum of the local moments. This might be connected to some novel mechanism (such as orbital magnetism) for the formation of these moments. There is a possibility that phonon excitation spectra and the coupling of the nuclei to the phonon bath get strongly modified in nanoparticles and are still effective in $1/T_1$. However, it seems unlikely that there are only ferromagnetic and diamagnetic regions in the sample without any paramagnetic ones. A theoretical effort is needed to understand better the phonons as also the dynamical susceptibility of defect induced moments in nanoparticles.

Conclusions. - We have probed a nanoparticulate sample of SnO_2 using bulk magnetisation and ^{119}Sn NMR measurements. While bulk data show hysteresis in the isothermal magnetisation with magnetic field, evidence of paramagnetic moments is seen in the ^{119}Sn NMR $1/T_1$ data. The nuclear magnetisation recovery follows a stretched exponential behaviour with the stretching exponent $\beta \sim 0.75$ which is nearly T -independent. The relaxation rate is strongly enhanced in the nano sample in comparison to the bulk. A 15% loss of the NMR signal in the nano as compared to the bulk is thought to be from static local moments (due to ferromagnetism) in a part of the sample which shift the NMR signal out of our window of observation.

We thank Department of Science and Technology, Govt. of India for financial support.

-
- [1] OHNO H., *Science*, **281** (1998) 951.
[2] DIETL T., OHNO H., MATSUKURA F., CIBERT J. AND FERRAND D., *Science*, **287** (2000) 1019.
[3] MATSUMOTO Y., MURAKAMI M., SHONO T., HASEGAWA T., FUKUMURA T., KAWASAKI M., AHMET P., CHIKYOW T., KOSHIHARA S. AND KOINUMA H., *Science*, **291** (2001) 854.
[4] SHARMA P., GUPTA A., RAO K. V., OWENS F. J., SHARMA R., AHUJA R., GUILLEN J. M. O., JOHANSSON B. AND GEHRING G. A., *Nat. Mater.*, **2** (2003) 673.
[5] HONG N. H., SAKAI J., HUONG N. T. AND BRIZÉ V., *Appl. Phys. Lett.*, **87** (2005) 102505.
[6] OGALE S. B., CHOUDHARY R. J., BUBAN J. P., LOFLAND S. E., SHINDE S. R., KALE S. N., KULKARNI V. N., HIGGINS J., LANCI C., SIMPSON J. R., BROWNING N. D., DAS SARMA S., DREW H. D., GREENE R. L. AND VENKATESAN T., *Phys. Rev. Lett.*, **91** (2003) 077205.
[7] TIWARI A., BHOSLE V. M., RAMACHANDRAN S., SUDHAKAR N., NARAYAN J., BUDAK S. AND GUPTA A., *Appl. Phys. Lett.*, **88** (2006) 142511.
[8] VENKATESAN M., FITZGERALD C. B. AND COEY J. M. D., *Nature London*, **430** (2004) 630.
[9] SUNDARESAN A., BHARGAVI R., RANGARAJAN N., SIDDESH U. AND RAO C. N. R., *Phys. Rev. B*, **74** (2006) 161306(R).
[10] HONG N. H., SAKAI J., POIROT N. AND BRIZÉ V., *Phys. Rev. B*, **73** (2006) 132404.
[11] BANERJEE S., MANDAL M., GAYATHRI N. AND SARDAR M., *Appl. Phys. Lett.*, **91** (2007) 182501.
[12] GANGULI N., DASGUPTA I. AND SANYAL B., *J. Appl. Phys.*, **108** (2010) 123911.
[13] RAHMAN G., GARCÍA-SUÁREZ V. M. AND HONG S. C., *Phys. Rev. B*, **78** (2008) 184404.
[14] WANG H., YAN Y., LI K., DU X., LAN Z. AND JIN H., *Phys. Status Solidi B*, **247** (2010) 444.
[15] SABARINATHAN V., VINOD CHANDRAN C., RAMASAMY S. AND GANAPATHY S., *Journal of Nanoscience and Nanotechnology*, **8** (2008) 321.
[16] TANG H.-Y., LIN C.-C., WANG L.-S., YANG W.-C., LIAO K.-H., LI F.-Y. AND LIAO M.-Y., *Phys. Rev. B*, **77** (2008) 165420.
[17] TOMASELLI M., YARGER J. L., BRUCHEZ, JR. M., HAVLIN R. H., DEGRAW D., PINES A., AND ALIVISATOS A. P., *J. Chem. Phys.*, **110** (1999) 8861.
[18] MONREDON S. DE, CELLOT A., RIBOT F., SANCHEZ C., ARMELAO L., GUENEAU L. AND DELATTRE L., *J. Mater. Chem.*, **12** (2002) 2396.
[19] THE LONGEST DELAY ' t ' USED BY THEM IN THE $\pi/2 - t - (\pi/2 - \pi)$ SEQUENCE IS MUCH SMALLER THAN THE T_1 .
[20] GNANAM S. AND RAJENDRAN V., *J Sol-Gel Sci Technol.*, **53** (2009) 555.

[21] KOJIMA K., HUKUDA Y., KAWANAKA H., TAKABATAKE T., FUJII H. AND HIHARA T., *Journal of Magnetism and*

Magnetic Materials, **90-91** (1990) 505.